

Testing the Higgs model with triplet fields at the ILC *

Kei Yagyu

Department of Physics, University of Toyama, 3190 Gofuku, Toyama 930-8555, Japan

Higgs triplet fields are introduced various new physics models such as the type-II seesaw model, the left-right symmetric model and so on. The vertex of a charged Higgs boson and weak gauge bosons, $H^\pm W^\mp Z$, appears at the tree level in these models. The magnitude of this vertex is proportional to the vacuum expectation value (VEV) of Higgs triplet fields. We discuss the possibility of measuring this vertex at the ILC and study how precisely determine the VEV of the triplet field.

1 Introduction

The Higgs sector is the last unknown part of the Standard Model (SM). The Higgs sector may not necessarily be the minimal form in the SM. Extended Higgs sectors have often been considered in various new physics contexts beyond the SM. Therefore, determination of the Higgs sector is important to obtain a clue to new physics at the TeV scale.

An important observable to constrain the structure of extended Higgs models is the electroweak rho parameter ρ , whose experimental value is very close to unity. This fact suggests that a global $SU(2)$ symmetry (custodial symmetry) plays an important role in the Higgs sector. In the Higgs model which contains complex scalar fields with the isospin T_i and the hypercharge Y_i as well as real ($Y = 0$) scalar fields with the isospin T'_i , the rho parameter is given at the tree level by

$$\rho_{\text{tree}} = \frac{\sum_i [|v_i|^2(T_i(T_i + 1) - Y_i^2) + u_i^2 T'_i(T'_i + 1)]}{2 \sum_i |v_i|^2 Y_i^2}, \quad (1)$$

where v_i (u_i) represents the vacuum expectation value (VEV) of the complex (real) scalar field [2]. In the model with only scalar doublet fields (and singlets), we obtain $\rho_{\text{tree}} = 1$ so that the natural extension of the Higgs sector is attained by adding extra doublet fields and singlet fields. On the other hand, addition of the Higgs field with the isospin larger than one half can shift the rho parameter from unity at the tree level, whose deviation is proportional to the VEVs of these exotic scalar fields. The rho parameter, therefore, has been used to exclude or to constrain a class of Higgs models.

A common feature in the extended Higgs models is the appearance of physical charged Higgs boson H^\pm . Hence, we may be able to discriminate each Higgs model through the physics of charged Higgs bosons. In particular, the $H^\pm W^\mp Z$ vertex can be a useful probe of the extended Higgs sector [3–6]. Assuming that there are several physical charged scalar states H_α^\pm ($\alpha \geq 2$) and the Nambu-Goldstone modes H_1^\pm , the vertex parameter ξ_α in $\mathcal{L} = igm_W \xi_\alpha H_\alpha^\pm W^- Z + \text{h.c.}$ is calculated at the tree level as [3]

$$\sum_{\alpha \geq 2} |\xi_\alpha|^2 = \frac{1}{\cos^2 \theta_W} \left[\frac{2g^2}{m_W^2} \left\{ \sum_i [T_i(T_i + 1) - Y_i^2] |v_i|^2 Y_i^2 \right\} - \frac{1}{\rho_{\text{tree}}^2} \right], \quad (2)$$

*This proceedings is based on Ref. [1].

where ρ_{tree} is given in Eq. (1). A non-zero value of ξ_α appears at the tree level only when H_α^\pm comes from an exotic representation such as triplets. Similarly to the case of the rho parameter, the vertex is related to the custodial symmetry. In general, this can be independent of the rho parameter. Therefore, the measurement of the $H^\pm W^\mp Z$ vertex can be a complementary tool to the rho parameter in testing the *exoticness* of the Higgs sector. At LHC, the possibility of measuring the $H^\pm W^\mp Z$ vertex has been studied [8].

In this talk, we discuss the possibility of measuring the $H^\pm W^\mp Z$ vertex via the process $e^+e^- \rightarrow H^\pm W^\mp$ at the International Linear Collider (ILC) [9–11] by using the recoil method. The feasibility of the signal $e^+e^- \rightarrow H^\pm W^\mp \rightarrow \ell\nu jj$ is analyzed assuming the polarized electron and positron beams and the expected detector performance for the resolution of the two-jet system at the ILC, where decay of H^\pm are assumed to be lepton specific [12]. The background events can be reduced to a considerable extent by imposing the kinematic cuts even if we take into account the initial state radiation (ISR).

2 The $H^\pm W^\mp Z$ vertex and the process $e^+e^- \rightarrow H^\pm W^\mp$

The $H^\pm W^\mp Z$ vertex ^a is defined in FIG. 1, where $V^{\mu\nu}$ is expressed in terms of the form factors F_{HWZ} , G_{HWZ} and H_{HWZ} as

$$V^{\mu\nu} = F_{HWZ}g^{\mu\nu} + G_{HWZ}\frac{p_W^\mu p_Z^\nu}{m_W^2} + iH_{HWZ}\frac{p_{W\rho} p_{Z\sigma}}{m_W^2}\epsilon^{\mu\nu\rho\sigma}, \quad (3)$$

with $\epsilon_{\mu\nu\rho\sigma}$ being the anti-symmetric tensor, and p_Z^μ and p_W^μ being the outgoing momenta of Z and W bosons, respectively. The form factors G_{HWZ} and H_{HWZ} are related to the coefficients of the dimension five operator in the Lagrangian [4, 5], while F_{HWZ} is related to those of the dimension three operator, so that only F_{HWZ} may appear at the tree level. Therefore, the dominant contribution to the $H^\pm W^\mp Z$ vertex is expected to be from F_{HWZ} .

In the Higgs model with only doublet scalar fields (plus singlets) all the form factors including F_{HWZ} vanish at the tree level [3], because of the custodial invariance in the kinetic term. The form factors F_{HWZ} , G_{HWZ} and H_{HWZ} are generally induced at the loop level. On the other hand, in models with Higgs triplet fields, the $H^\pm W^\mp Z$ vertex appears at the tree level. In the model with an isospin doublet field ($Y = 1/2$) and either a real triplet field η ($Y = 0$) or an additional complex triplet field Δ ($Y = 1$), concrete expressions for the tree-level formulae for $|F_{HWZ}|^2$ and that of ρ_{tree} are shown in TABLE 1, where v , v_η and v_Δ are respectively VEVs of the doublet scalar field and the additional triplet scalar fields η and Δ . These triplet scalar fields also contribute to the rho parameter at the tree level, so that their VEVs are constrained by the current rho parameter data, $\rho_{\text{exp}} = 1.0008^{+0.0017}_{-0.0007}$ [7]; i.e., $v_\eta \lesssim 6$ GeV for the VEV of η , and $v_\Delta \lesssim 8$ GeV for that of Δ (95 % CL). We note that in order to

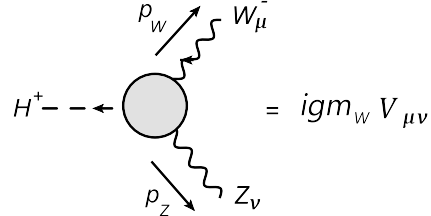


Figure 1: The $H^\pm W^\mp Z$ vertex.

^aThe $H^\pm W^\mp \gamma$ vertex vanishes at the tree level due to the $U(1)_{\text{em}}$ gauge invariance in any extended Higgs models [4].

Model	SM with η ($Y = 0$)	SM with Δ ($Y = 1$)	the GM model
$ F_{HWZ} ^2 =$	$\frac{4v^2 v_\eta^2}{\cos^2 \theta_W (v^2 + 4v_\eta^2)^2}$	$\frac{2v^2 v_\Delta^2}{\cos^2 \theta_W (v^2 + 2v_\Delta^2)^2}$	$\frac{4v_\Delta^2}{\cos^2 \theta_W (v^2 + 4v_\Delta^2)}$
$\rho_{\text{tree}} =$	$1 + \frac{4v_\eta^2}{v^2}$	$\frac{1 + 2\frac{v_\Delta^2}{v^2}}{1 + 4\frac{v_\Delta^2}{v^2}}$	1

Table 1: The tree-level expression for F_{HWZ} and rho parameter in the model with a real triplet field η , that with a complex triplet field Δ and the Georgi-Machacek (GM) model [13].

obtain the similar accuracy to the rho parameter data by measuring the $H^\pm W^\mp Z$ vertex, the vertex has to be measured with the detectability to $|F_{HWZ}|^2 \sim \mathcal{O}(10^{-3})$.

Finally, we mention the model with η and Δ in addition to the SM, which is proposed by Georgi-Machacek and Chanowiz-Golden [13–15]. In this model, an alignment of the VEVs for η and Δ are introduced ($v_\eta = v_\Delta/\sqrt{2}$), by which the Higgs potential is invariant under the custodial symmetry at the tree level. Physical scalar states in this model can be classified using the transformation property against the custodial symmetry; i.e., the five-plet, the three-plet and the singlet. Only the charged Higgs boson from the five-plet state has the non-zero value of F_{HWZ} at the tree level. Its value is proportional to v_Δ . However, the value of v_Δ is not strongly constrained by the rho parameter data, because the tree level contribution to the rho parameter is zero due to the custodial symmetry: see TABLE 1. Consequently, the magnitude of $|F_{HWZ}|^2$ can be of order one.

The process $e^+e^- \rightarrow Z^* \rightarrow H^-W^+$ is directly related to the $H^\pm W^\mp Z$ vertex. The helicity specified cross sections of the process are calculated as a function of the center-of-mass energy \sqrt{s} and the helicity of the electron τ [10];

$$\sigma(s; \tau) = \frac{1}{32\pi s} \beta \left(\frac{m_{H^\pm}^2}{s}, \frac{m_W^2}{s} \right) \int_{-1}^1 d \cos \theta |\mathcal{M}(\tau)|^2, \quad (4)$$

where θ and m_{H^\pm} are the angle between the momentum of H^\pm and the beam axis and the mass of H^\pm . The function $\beta(x, y)$ is

$$\beta(x, y) = \sqrt{1 + x^2 + y^2 - 2xy - 2x - 2y}. \quad (5)$$

The squared amplitude $|\mathcal{M}(\tau)|^2$ can be written as

$$|\mathcal{M}(\tau)|^2 = g^2 C_Z^2 \frac{|F_{HWZ}|^2}{(s - m_Z^2)^2} \left[\frac{\sin^2 \theta}{4} (s + m_W^2 - m_{H^\pm}^2)^2 + s m_W^2 (\cos^2 \theta + 1) \right], \quad (6)$$

where the form factors G_{HWZ} and H_{HWZ} are taken to be zero and

$$C_Z = \frac{g}{\cos \theta_W} (T_e^3 + \sin^2 \theta_W), \quad T_e^3 = \begin{cases} -1/2 & \text{for } \tau = -1, \\ 0 & \text{for } \tau = +1 \end{cases}. \quad (7)$$

In FIG. 2, we show that the \sqrt{s} dependence of the helicity dependent and the helicity averaged cross sections.

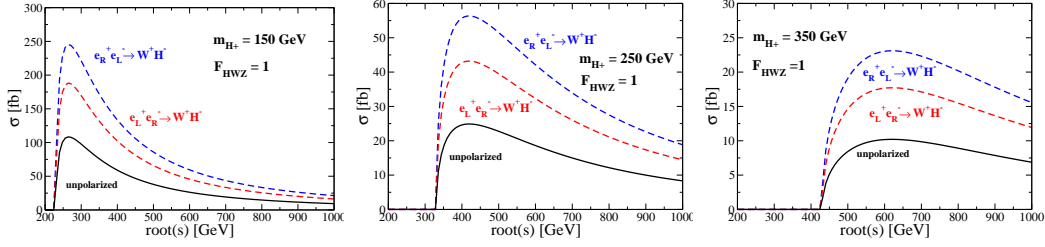


Figure 2: The total cross section of $e^+e^- \rightarrow W^+H^-$ as a function of \sqrt{s} in the case of $F_{HWZ} = 1$.

3 The signal and background analysis

We investigate the possibility of measuring the $H^\pm W^\mp Z$ vertex by using a recoil method [17] at the ILC. In order to identify the process, we consider the hadronic decays $W \rightarrow jj$ instead of the leptonic decay of the produced W boson. The recoiled mass of H^\pm is given in terms of the two-jet energy E_{jj} and the two-jet invariant mass M_{jj} as

$$m_{\text{recoil}}^2(jj) = s - 2\sqrt{s}E_{jj} + M_{jj}^2. \quad (8)$$

It is clear that the detector performance for the resolution of two jets is crucial in such an analysis. In particular, the jets from the W boson in the signal process have to be precisely measured in order to be separated with those from the Z boson in the background process. At the ILC, the resolution for the two jet system with the energy E in the unit of GeV is expected to be $\sigma_E = 0.3\sqrt{E}$ GeV, by which the background from $Z \rightarrow jj$ can be considerably reduced. We here adopt the similar value for $\sigma_E=3$ GeV in our later analysis.

At the ILC, the polarized electron and positron beams can be used, by which the background from the W boson pair production process can be reduced. We here use the following beams polarized as

$$\frac{N_{e_R^-} - N_{e_L^-}}{N_{e_L^-} + N_{e_R^-}} = 0.8, \quad \frac{N_{e_L^+} - N_{e_R^+}}{N_{e_L^+} + N_{e_R^+}} = 0.5, \quad (9)$$

which are expected to be attained at the ILC [16], where $N_{e_{R,L}^-}$ and $N_{e_{R,L}^+}$ are numbers of right- (left-) handed electron and positron in the beam flux per unit time.

First, we discuss the case without the effect of the ISR, and after that we discuss the case with the ISR. The size of the signal cross section is determined by \sqrt{s} , m_{H^\pm} and F_{HWZ} . In order to examine the possibility of constraining $|F_{HWZ}|^2$, we here assume that m_{H^\pm} is already known with some accuracy by measuring the other processes at the LHC or at the ILC. Then $|F_{HWZ}|^2$ is the only free parameter in the production cross section.

In order to perform the signal and background analysis, we assume that the decay of the produced H^\pm is lepton specific; i.e., $H^\pm \rightarrow \ell\nu$ where ℓ is either e , μ or τ . The final state of the signal is then $e^+e^- \rightarrow H^\pm W^\mp \rightarrow \ell\nu jj$. The main backgrounds come from the W boson pair production process $e^+e^- \rightarrow W^+W^-$ and the single W production processes $e^+e^- \rightarrow Z^*/\gamma^* \rightarrow W^\pm jj$ and $e^+e^- \rightarrow Z^*/\gamma^* \rightarrow W^\pm \ell^\mp \nu$. For the $e^\pm \nu jj$ final state,

	Basic	M_{jj}	p_T^{jj}	E_{jj}	$\cos\theta_{\text{lep}}$	$M_{\ell\nu}$
Signal (fb)	0.15	0.14	8.9×10^{-2}	8.9×10^{-2}	7.0×10^{-2}	7.0×10^{-2}
$\ell\nu jj$ background (fb)	820	720	120	7.4	1.5	8.0×10^{-1}
$\ell\ell jj$ background (fb)	330	5.2	3.0×10^{-1}	2.5×10^{-2}	1.2×10^{-2}	6.4×10^{-3}
S/\sqrt{B}	0.14	0.16	0.26	1.0	1.8	2.5

Table 2: The results without the ISR. The signal and the backgrounds cross sections are shown for $\sqrt{s} = 300$ GeV. For the signal, m_{H^\pm} is 150 GeV and $|F_{HWZ}|^2$ is taken to be 10^{-3} . For the $\ell\ell jj$ processes, the misidentity rate of one of the leptons is assumed to be 0.1. The signal significance S/\sqrt{B} are evaluated for the integrated luminosity to be 1 ab^{-1} .

	Basic	M_{jj}	p_T^{jj}	E_{jj}	$\cos\theta_{\text{lep}}$	$M_{\ell\nu}$
Signal (fb)	0.14	0.13	6.9×10^{-2}	6.6×10^{-2}	5.2×10^{-2}	5.1×10^{-2}
$\ell\nu jj$ background (fb)	810	720	130	13	6.2	6.7×10^{-1}
$\ell\ell jj$ background (fb)	360	4.6	0.29	3.4×10^{-2}	2.1×10^{-2}	5.5×10^{-3}
S/\sqrt{B}	0.13	0.15	0.19	5.8×10^{-1}	6.6×10^{-1}	2.0

Table 3: The results with the ISR. The signal and the backgrounds cross sections are shown for $\sqrt{s} = 300$ GeV. For the signal, m_{H^\pm} is 150 GeV and $|F_{HWZ}|^2$ is taken to be 10^{-3} . For the $\ell\ell jj$ processes, the misidentity rate of one of the leptons is assumed to be 0.1. The signal significance S/\sqrt{B} are evaluated for the integrated luminosity to be 1 ab^{-1} .

additional processes $e^+e^- \rightarrow e^\pm\nu W^{\mp*}$, $e^+e^- \rightarrow e^\pm\nu W^{\mp*}Z^*$ and $e^+e^- \rightarrow e^\pm\nu W^{\mp*}\gamma^*$ can also be significant backgrounds. In addition, we take into account the processes with the final state of $\ell\ell jj$. They can be backgrounds if one of the outgoing leptons escapes from the detection at the detector. We assume that the efficiency for lepton identification is 90 %.

We impose the basic cuts for all events such as

$$10^\circ < A_j < 170^\circ, \quad 5^\circ < A_{jj} < 175^\circ, \quad 10 \text{ GeV} < E_{jj}, \quad (10)$$

where A_j is the angle between a jet and the beam axis, A_{jj} is the angle between the two jets and E_{jj} is the energy of the two jets. In the numerical evaluation, we use CalcHEP [18]. After the basic cuts, the cross section for the signal is 0.15 fb and that for the background is 1.2 pb, where we set $\sqrt{s} = 300$ GeV, $m_{H^\pm} = 150$ GeV and $|F_{HWZ}|^2 = 10^{-3}$. In order to improve the signal over background ratio, we impose additional kinematic cuts. The two jets come from the W boson for the signal, so that the following invariant mass cut is useful to reduce the backgrounds;

$$m_W - 2\sigma_E < M_{jj} < m_W + 2\sigma_E. \quad (11)$$

In FIG. 3, the differential cross sections of the signal and the backgrounds are shown for the events after the M_{jj} cut in Eq. (11) as a function of the transverse momentum p_T^{jj} , the energy of the jj system, the angle θ_{lep} of a charged lepton with the beam axis, and the

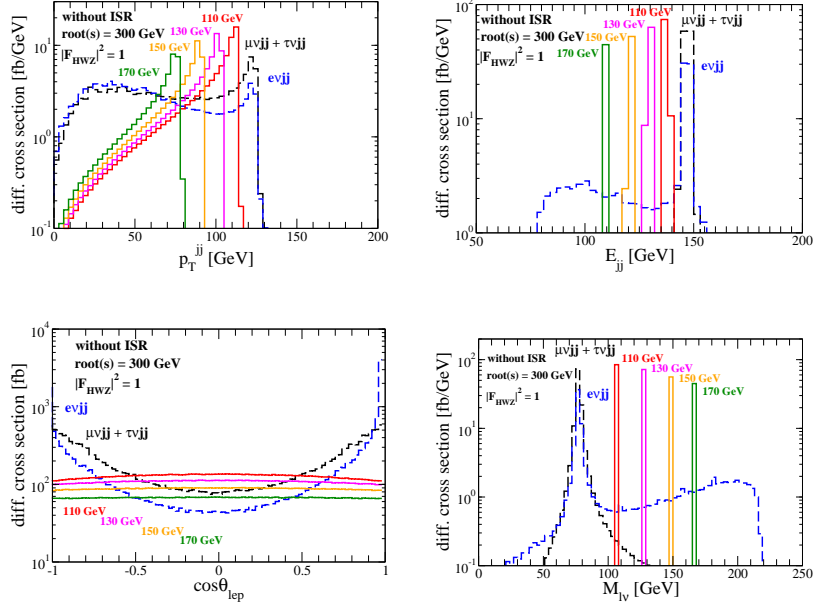


Figure 3: Distributions of the signal for $m_{H^\pm} = 110, 130, 150$ and 170 GeV as well as the backgrounds after M_{jj} cut in Eq. (11) without the ISR as a function of the transverse momentum p_T^{jj} (upper left), the energy of the jj system (upper right), the angle θ_{lep} of a charged lepton with the beam axis (lower left), and the invariant mass $M_{\ell\nu}$ of the charged lepton and the missing momentum in the final state (lower right). $|F_{HWZ}|^2$ is taken to be 1.

invariant mass $M_{\ell\nu}$ of the charged lepton and the missing momentum in the final state. For the signal, the results are shown for $|F_{HWZ}|^2 = 1$ with m_{H^\pm} to be 110, 130, 150 and 170 GeV.

In the following, we discuss the case with $m_{H^\pm} = 150$ GeV. According to FIG. 3, we impose the following four kinematic cuts sequentially:

$$75 \text{ GeV} < p_T^{jj} < 100 \text{ GeV} \quad \text{and} \quad 115 \text{ GeV} < E_{jj} < 125 \text{ GeV}, \quad (12)$$

for the jj system in the final state. In TABLE 2, the resulting values for the cross sections for the signal and backgrounds are shown in each step of the cuts. For $|F_{HWZ}|^2 = 10^{-3}$, the signal significance reaches to $\mathcal{O}(1)$ assuming the integrated luminosity of 1 ab^{-1} .

Until now, we have imposed the cuts on the jj system, and no information from the $\ell\nu$ system has been used. Here, in order to further improve the signal significance, we impose new cuts related to the $\ell\nu$ system in order, which are determined from FIG. 3;

$$|\cos \theta_{\text{lep}}| < 0.75 \quad \text{and} \quad 144 \text{ GeV} < M_{\ell\nu} < 156 \text{ GeV}. \quad (13)$$

As shown in TABLE 2, for $|F_{HWZ}|^2 = 10^{-3}$ the signal significance after these cuts can reach to $S/\sqrt{B} \simeq 2.5$ assuming the integrated luminosity of 1 ab^{-1} .

Next let us see how this results can be changed by including the ISR. We use the beam

Model	SM with η ($Y = 0$)	SM with Δ ($Y = 1$)	the GM model
ρ_{exp} with 95% CL	$v_\eta < 6$ GeV	$v_\Delta < 8$ GeV	-
$ F_{HWZ} ^2 < 10^{-3}$	$v_\eta < 3$ GeV	$v_\Delta < 4$ GeV	$v_\Delta < 3$ GeV

Table 4: The upper bound for the VEVs of the triplet field from the constraint by the rho parameter data with 95% CL and $|F_{HWZ}|^2 < 10^{-3}$.

parameters which are defined in CalcHEP [18] as the default value^b. The biggest change can be seen in the E_{jj} distribution. The background events in the E_{jj} distribution originally located at the point just below 150 GeV in the case without the ISR, which corresponds to the W boson mass. This tends to move in the lower E_{jj} regions, so that the signal over background ratio becomes worse. In TABLE 3, the resulting values for the cross sections for the signal and backgrounds are shown in each step of the cuts. Consequently, the signal significance after all the cuts is smeared from 2.5 to 2.0. We stress that even taking the ISR into account, the $H^\pm W^\mp Z$ vertex with $|F_{HWZ}|^2 > 10^{-3}$ can be excluded with 95% CL.

In the above analysis, we have assumed the lepton specific H^\pm scenario, where H^\pm decay into $\ell\nu$, and we have not specified the branching fractions of $B(H^\pm \rightarrow e^\pm\nu)$, $B(H^\pm \rightarrow \mu^\pm\nu)$ and $B(H^\pm \rightarrow \tau^\pm\nu)$ which depend on details of each Higgs model. If we assume $B(H^\pm \rightarrow e^\pm\nu) = 1$, the signal cross section does not change from the result shown in Table 3, while the background becomes 70 % of all the $\ell\nu jj$ background as evaluated from Table 3. As the result, the signal significance S/\sqrt{B} becomes about 2.4 in the case with the ISR for $|F_{HWZ}|^2 = 10^{-3}$. Similarly, If we assume $B(H^\pm \rightarrow \mu^\pm\nu) = 1$, the signal cross section does not change from the result shown in Table 3, while the background becomes 15 % of all the $\ell\nu jj$ background. Thus, the signal significance S/\sqrt{B} becomes about 5.0 in the case with the ISR for $|F_{HWZ}|^2 = 10^{-3}$.

Finally, we discuss the upper bound for the VEVs of the triplet fields. The constraint for $|F_{HWZ}|^2$ can be translated into that for the VEVs of the triplet fields (see Table 1). The upper bound for the VEVs of the triplet field are listed in Table 4 by the constraint from the rho parameter data with 95% CL and for $|F_{HWZ}|^2 < 10^{-3}$.

4 Conclusion

We have discussed the possibility of measuring the $H^\pm W^\mp Z$ vertex at the ILC. The vertex is important to understand the exoticness of the Higgs sector, so that the combined information of this vertex with the rho parameter provides a useful criterion to determine the structure of the extended Higgs sector. Assuming that the decay of the charged Higgs bosons is lepton specific, the feasibility of the vertex is analyzed by using the recoil method via the process $e^+e^- \rightarrow H^\pm W^\mp \rightarrow \ell\nu jj$ with the parton level simulation for the background reduction. We have found that the vertex with $|F_{HWZ}|^2 \geq \mathcal{O}(10^{-3})$ can be excluded with the 95% confidence level when $120\text{-}130 \text{ GeV} < m_{H^\pm} < m_W + m_Z$. The measurement of the $H^\pm W^\mp Z$ vertex with $|F_{HWZ}|^2 \geq \mathcal{O}(10^{-3})$ gives a precise information for the Higgs sector, whose accuracy is similar to that of the rho parameter.

^b We have confirmed that the results are almost unchanged even when we use the values given in Ref. [16].

Acknowledgments

I would like to thank Shinya Kanemura and Kazuya Yanase for fruitful collaborations. This work was supported by JSPS Fellow.

References

- [1] S. Kanemura, K. Yagyu, K. Yanase, *Phys. Rev.* **D83**, 075018 (2011).
- [2] J. F. Gunion, H. E. Haber, G. L. Kane and S. Dawson, “THE HIGGS HUNTER’S GUIDE,” *Front. Phys.* **80**, 1 (2000).
Phys. Rev. D **46**, 381 (1992).
- [3] J. A. Grifols and A. Mendez, *Phys. Rev. D* **22**, 1725 (1980); A.A. Iogansen, N.G. Ural'tsev, V.A. Khoze, *Sov. J. Nucl. Phys.* **36** 717 (1982).
- [4] A. Mendez and A. Pomarol, *Nucl. Phys. B* **349**, 369 (1991); M. C. Peyranere, H. E. Haber and P. Irulegui, *Phys. Rev. D* **44**, 191 (1991); J.L. Díaz-Cruz, J. Hernández-Sánchez, J.J. Toscano, *Phys. Lett. B* **512**, 339 (2001).
- [5] S. Kanemura, *Phys. Rev. D* **61**, 095001 (2000).
- [6] H. Haber, H. Logan, *Phys. Rev. D* **62**, 015011 (2000).
- [7] K. Nakamura, et al., (Particle Data Group), *J. Phys. G* **37**, 075021 (2010).
- [8] E. Asakawa and S. Kanemura, *Phys. Lett. B* **626**, 111 (2005); E. Asakawa, S. Kanemura and J. Kanzaki, *Phys. Rev. D* **75**, 075022 (2007); M. Battaglia, A. Ferrari, A. Kiiskinen, T. Maki, [hep-ex/0112015]; S. Godfrey, K. Moats, *Phys. Rev.* **D81**, 075026 (2010).
- [9] K. Cheung, R. J. N. Phillips and A. Pilaftsis, *Phys. Rev. D* **51**, 4731 (1995).
- [10] S. Kanemura, *Eur. Phys. J. C* **17**, 473 (2000); S. Kanemura, S. Moretti and K. Odagiri, *JHEP* **0102**, 011 (2001).
- [11] S.-H. Zhu, hep-ph/9901221; A. Arhrib, et al., *Nucl. Phys. B* **581**, 34 (2000); H.E. Logan, S. Su, *Phys. Rev. D* **66**, 035001 (2002); *Phys. Rev. D* **67**, 017703, (2003); O. Brein and T. Hahn, *Eur. Phys. J. C* **52**, 397 (2007); K. Cheung, R. Phillips, A. Pilaftsis, *Phys. Rev. D* **51**, 4731 (1995); R.M. Godbole, B. Mukhopadhyaya, M. Nowakowski, *Phys. Rev. D* **352**, 388 (1995); D.K. Ghosh, R.M. Godbole, B. Mukhopadhyaya, *Phys. Rev. D* **55**, 3150 (1997).
- [12] M. Aoki, S. Kanemura, K. Tsumura and K. Yagyu, *Phys. Rev. D* **80**, 015017 (2009); H. S. Goh, L. J. Hall and P. Kumar, *JHEP* **0905**, 097 (2009); S. Su and B. Thomas, *Phys. Rev. D* **79**, 095014 (2009); H. E. Logan and D. MacLennan, *Phys. Rev. D* **79**, 115022 (2009).
- [13] H. Georgi and M. Machacek, *Nucl. Phys. B* **262**, 463 (1985); M. S. Chanowitz and M. Golden, *Phys. Lett. B* **165**, 105 (1985).
- [14] J. F. Gunion, R. Vega and J. Wudka, *Phys. Rev. D* **42**, 1673 (1990); R. Vega and D. A. Dicus, *Nucl. Phys. B* **329**, 533 (1990). J. F. Gunion, R. Vega and J. Wudka, *Phys. Rev. D* **43**, 2322 (1991); R. Godbole, B. Mukhopadhyaya and M. Nowakowski, *Phys. Lett. B* **352**, 388 (1995).
- [15] M. Aoki and S. Kanemura, *Phys. Rev. D* **77**, 095009 (2008).
- [16] J. Brau, (Ed.) *et al.* [ILC Collaboration], [arXiv:0712.1950 [physics.acc-ph]]; G. Aarons *et al.* [ILC Collaboration], [arXiv:0709.1893 [hep-ph]]; T. Behnke, (Ed.) *et al.* [ILC Collaboration], [arXiv:0712.2356 [physics.ins-det]].
- [17] W. Lohmann, M. Ohlerich, A. Raspereza and A. Schalicke, *In the Proceedings of 2007 International Linear Collider Workshop (LCWS07 and ILC07), Hamburg, Germany, 30 May - 3 Jun 2007, pp TIG13* [arXiv:0710.2602 [hep-ex]]; H. Li, F. Richard, R. Poeschl and Z. Zhang, arXiv:0901.4893 [hep-ex].
- [18] A. Pukhov, [hep-ph/0412191].